Monatsh Chem 139, 349–362 (2008)
DOI 10.1007/s00706-007-0831-y
Printed in The Netherlands

Monatshefte für Chemie
Chemical Monthly

Theoretical investigation (DFT and *MP*2) of the intermolecular proton transfer in the supersystems uracil-$(H_2O)_n$ and uracil-$(CH_3OH)_n$ $(n = 1, 2)$

Vassil B. Delchev[1], Ivan G. Shterev[2], Hans Mikosch[3]

[1] Department of Physical Chemistry, University of Plovdiv, Plovdiv, Bulgaria
[2] Department of Physical and Inorganic Chemistry, University of Food Technologies, Plovdiv, Bulgaria
[3] Institute of Chemical Technologies and Analytics, Technical University Vienna, Wien, Austria

Received 10 September 2007; Accepted 18 October 2007;

Abstract Twelve binary and eight ternary H-bonded systems between uracil and water/methanol were investigated at the *B3LYP* and *MP*2 theoretical levels using $6-31+G(\mathrm{d})$ basis functions. The binary and ternary systems that contain the hydroxo-uracil tautomer H-bonded with water and methanol were found to be the most stable complexes. The calculated energy barriers of the intermolecular proton exchange showed that the methanol molecule provokes larger reduction of the energy barrier of the intermolecular proton exchange reactions than the water molecule.

Keywords DFT calculations; Energy barriers; H-Bonding; *MP*2 calculations; Uracil.

Introduction

Nucleic acid bases are elementary building blocks of *DNA* and *RNA*, which have always been the subject of numerous theoretical [1–6] and experimental [7–10] or combined [11, 12] research studies. One of the more important *RNA* bases is uracil that is a pyrimidine derivative with functional groups (hydroxo- or oxo-) at positions 2 and 6. The H-bonding between nucleic acid bases and other protic molecules has interested scientists for a long time. For example, the hydrogen bonded complexes between uracil and HCl have been studied by *Latajka et al.* [13] at the *HF* level of theory. The found interaction energies of the uracil-HCl complexes have shown a strong basis set dependence. They have provided no evidence for a significant difference between the two carbonyl groups in terms of intrinsic properties.

Bao et al. [14] have studied recently the uracil-water complexes *U*-$(H_2O)_n$ ($n = 1, 2$, and 3) at *B3LYP* theoretical level. The lowest energy has been calculated for the oxo-uracil tautomer H-bonded with water at C2=O and N3–H positions. Unfortunately, H-bonding and thermodynamic analysis of the complex stability has not been performed. In this aspect, it could not be explained whether the stability of this monohydrated complex comes from the highest stability of the oxo-uracil monomer or because of other reasons.

Empirical, quantum chemical calculations, and molecular dynamics simulations of the solvent influence on tautomerism in nucleic acid bases and their pairs have been summarized [15]. It has been demonstrated the strong influence of a solvent on the tautomeric equilibrium between the tautomers of bases and on the spatial arrangement of the bases in a base pair. The results have provided clear evidence that the prevalence of either the stacked or hydrogen-bonded structures of the base pairs in the solvent is not determined only by its bulk properties, but rather

---

Correspondence: Vassil B. Delchev, Department of Physical Chemistry, University of Plovdiv, Plovdiv, Bulgaria. E-mail: vdelchev@pu.acad.bg

by specific hydrophilic interactions of the base pair with a small number of solvent molecules [15]. Another investigation [16] has revealed that the energy surface of intermolecular proton transfers can be well reproduced when the assisted water molecules are replaced by point charges, but at close distances the charges need to be enhanced to account for induced polarization.

The crystal structure of uracil has been established long ago by diffraction [17, 18]. It has been reported that the oxo-uracil tautomer seems to be the most stable and abundant one in the solid state. However, in the liquid phase (especially in protic solvents) a fast proton exchange is expected. As a result new tautomeric forms could be obtained. The purpose of the current paper is a study of the possibility of uracil to tautomerize interacting with the solvent molecules (water, methanol in this research) through H-bonds. All the discussions and conclusions will be made only for ground states.

Discussion

Our preliminary investigations on the X-ray powder spectra of uracil (FLUKA), and uracil precrystallized from methanol and water showed a change in the crystal lattice of uracil after precrystallization: major diffraction peaks appear at $d = 3.135$, 3.148, and 3.127 Å. Obviously, water and methanol are included in the crystal lattice where water molecules serve as a linking compound between the lattice planes. As a result the distance (d) between the planes is reduced as compared to pure uracil. Of course, the methanol molecule does not have such behavior and its H-bonding (only with the OH group) to uracil provokes an elongation of d. These preliminary experiments explicitly prove that uracil forms strong H-bonds with water and methanol.

Twelve H-bonded supersystems composed of two monomers were studied from the standpoint of their stability and mechanism of intermolecular H-exchange. Their optimized structures are shown in Fig. 1 and the calculated energies and thermodynamic parameters are listed in Table 1.

The data in Table 1 unambiguously show that the supersystems C_{W1} and C_{M1} have the lowest energy. Perhaps this is a result of the highest stability of the oxo-uracil monomer [21]. According to the *B3LYP* optimizations this monomer is 56 kJ mol^{-1} more stable than the 6-hydroxo-uracil one, 52 kJ mol^{-1} than 2-hydroxo-uracil, and 65 kJ mol^{-1} than 2,6-dihydroxo-uracil.

The *B3LYP* functional is a reasonable choice for studying such H-bonded supersystems, the more so as several investigations of aromatic systems have revealed that geometries and frequencies of the molecules calculated at the *B3LYP* level agree well with experiment [19, 20, 22]. The lowest energy of the supersystem C_{W1} has been calculated by *Bao et al.* [14] also. Furthermore, they have shown that the energy difference between the complexes A_{w1} and C_{w1} calculated at the *B3LYP*/DZP++ level is 6.9 kJ mol^{-1} [14] whereas the value resulting from the *B3LYP*/$6-31+G$(d) calculations is 7.4 kJ mol^{-1} (the same value was predicted by the *MP*2 calculations as well). This insignificant difference, obviously provoked by the basis set, confirms the reliability of the basis set chosen for the calculations here. Unfortunately, in this study there is a gap on the ground state mechanism of proton exchange between water and uracil monomer as well as an investigation of the possible complexes of uracil with methanol.

The calculated energies (Table 1) of the binary supersystems follow the pattern: $C_{W/M1} < A_{W/M1} < E_{W/M1} < D_{W/M1} < B_{W/M1} < F_{W/M1}$ (*B3LYP* and *MP*2).

The calculated frequencies of the intermolecular vibrations (ν_i) of the binary supersystems, at the *MP*2 level, are in the interval 168–223 cm^{-1} (*B3LYP*: 164–223 cm^{-1}). It was established that the *MP*2 values of ν_i for the binary supersystems with water are lower than those calculated with the *B3LYP* functional. Conversely, for the methanol containing ones – the *MP*2 method predicted higher values of ν_i as compared to the *B3LYP* resulted frequencies.

The application of the *Onsager* continuum model (*B3LYP*) for the solvent effect prediction in the uracil-H_2O and uracil-CH_3OH in an appropriate environment led to a lowering of the energies of the supersystems with about 10 kJ mol^{-1} in the first case and 9 kJ mol^{-1} in the second case. These small energy reductions were expected since almost all continuum models, by nature, take in account only the electrostatic interactions between a certain molecule and its environment. That is why the H-bonded systems studied here pretend to reveal partially the discrete interactions between the uracil molecule and the surrounding medium (solvent). This is the first problem of the paper. The uracil molecules participate in dynamic interactions with environment, which include proton exchanges. Thus the mechan-

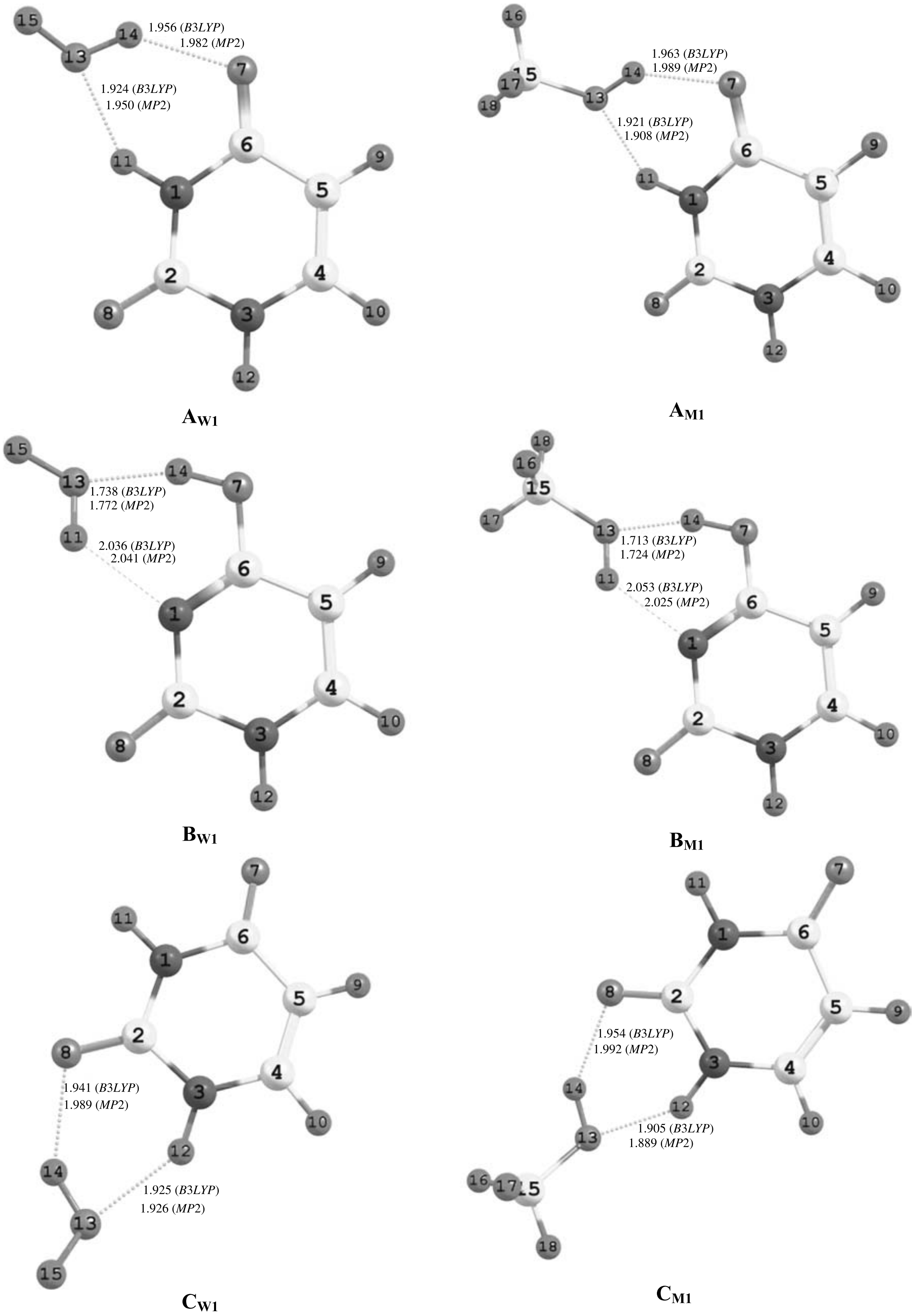

$\mathbf{A_{W1}}$ $\mathbf{A_{M1}}$

$\mathbf{B_{W1}}$ $\mathbf{B_{M1}}$

$\mathbf{C_{W1}}$ $\mathbf{C_{M1}}$

Fig. 1 Optimized structures of the binary supersystems

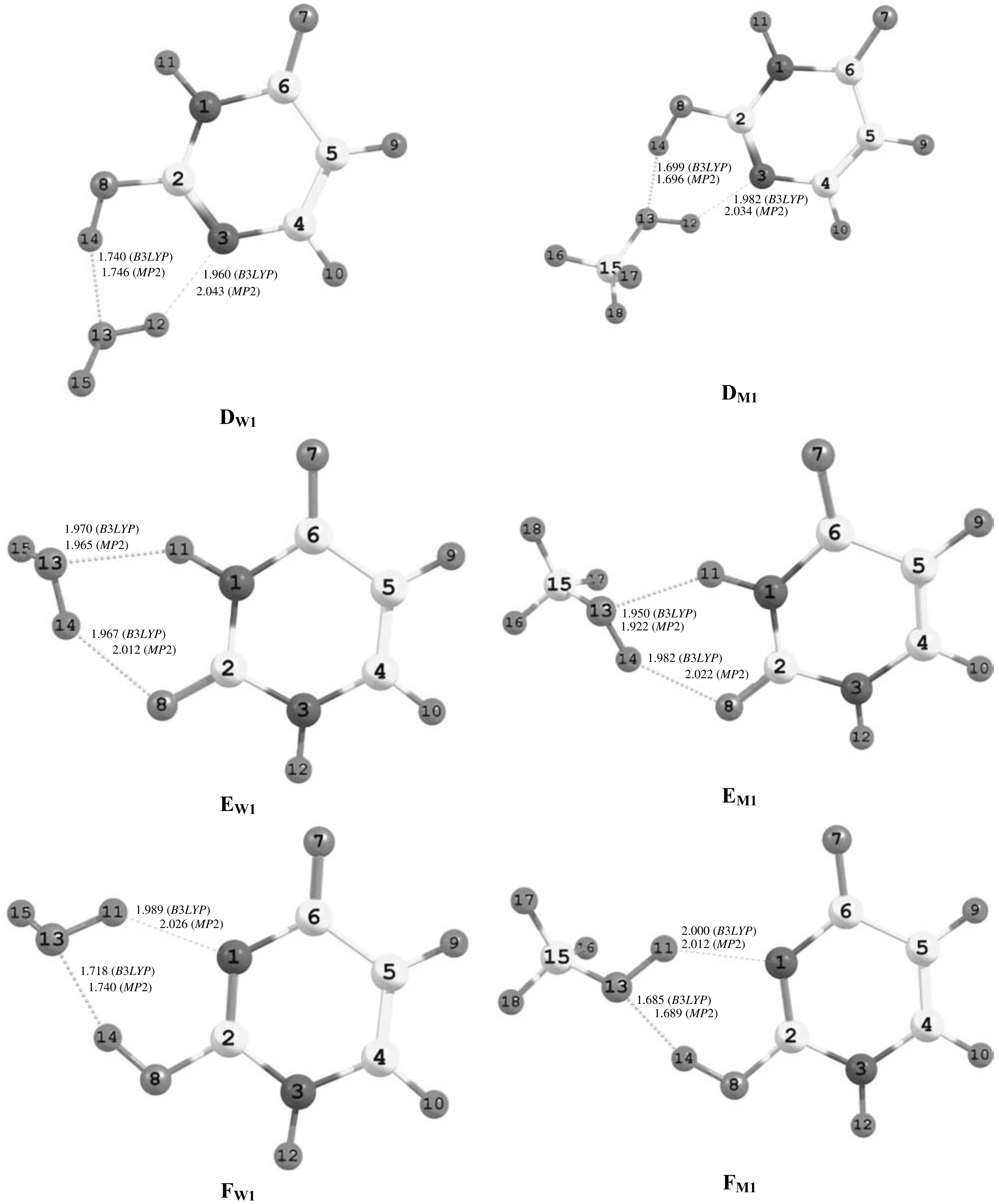

D_{W1} D_{M1}

E_{W1} E_{M1}

F_{W1} F_{M1}

Fig. 1 (*continued*)

ism of intermolecular H-transfer is very important to be known. Its study comprises the second main problem of the paper. However, this is a very challenging task for every computational chemist since there are several limitations. The first one is connected with the size of the molecular system to be

Table 1 Calculated energies and thermodynamic functions of the supersystems/*Hartree*

Supersystems	E_{elect}		$E_o = E_{\mathrm{elec}} + ZPE$	$H = E^* + RT$	$G = H\text{-}TS$
	1	2			
Binary supersystems					
$\mathrm{A_{W1}}$	−491.275442	−489.888782	−491.163613	−491.153579	−491.197885
$\mathrm{B_{W1}}$	−491.258699	−489.873072	−491.147417	−491.137441	−491.181683
$\mathrm{C_{W1}}$	−491.278252	−489.891597	−491.166229	−491.156262	−491.200445
$\mathrm{D_{W1}}$	−491.260892	−489.874929	−491.148929	−491.139352	−491.182558
$\mathrm{E_{W1}}$	−491.274513	−489.888092	−491.162789	−491.152679	−491.197176
$\mathrm{F_{W1}}$	−491.249569	−489.864597	−491.138199	−491.128397	−491.172091
$\mathrm{A_{M1}}$	−530.577844	−529.037851	−530.436956	−530.425447	−530.474584
$\mathrm{B_{M1}}$	−530.562043	−529.022958	−530.421424	−530.410151	−530.458617
$\mathrm{C_{M1}}$	−530.580524	−529.040644	−530.439431	−530.427972	−530.477118
$\mathrm{D_{M1}}$	−530.563501	−529.025011	−530.422583	−530.411436	−530.459421
$\mathrm{E_{M1}}$	−530.576853	−529.037185	−530.436021	−530.424447	−530.473803
$\mathrm{F_{M1}}$	−530.552504	−529.014609	−530.412155	−530.400806	−530.449441
Ternary supersystems					
$\mathrm{A_{W2}}$	−567.716306	−566.118976	−567.579490	−567.566631	−567.617506
$\mathrm{B_{W2}}$	−567.700630	−566.104285	−567.564284	−567.551523	−567.602152
$\mathrm{C_{W2}}$	−567.699067	−566.104137	−567.562492	−567.549908	−567.600071
$\mathrm{D_{W2}}$	−567.694519	−566.100063	−567.557801	−567.545414	−567.595042
$\mathrm{A_{M2}}$	−646.320970	−644.417114	−646.126036	−646.110202	−646.170790
$\mathrm{B_{M2}}$	−646.306631	−644.403254	−646.111746	−646.096199	−646.156003
$\mathrm{C_{M2}}$	−646.305845	−644.403331	−646.111239	−646.095661	−646.155349
$\mathrm{D_{M2}}$	−646.299975	−644.399686	−646.105215	−646.089785	−646.149043

1 B3LYP/$6-31+G$(d); *2 MP*2/$6-31+G$(d), $E^* = E_o + E_{\mathrm{vib}} + E_{\mathrm{rot}} + E_{\mathrm{transl}}$ [29]

calculated with accurate quantum mechanical methods. As known the real interactions between a molecule and the environment include a great number of interacting molecules of environment (water and methanol as in this study) with the dissolved molecule (uracil). We decided to restrict this number up

Table 2 Dihedral angles of supersystems water/methanol – uracil

Dihedral angle/deg	Level	$\mathrm{A_{W1}}$	$\mathrm{B_{W1}}$	$\mathrm{C_{W1}}$	$\mathrm{D_{W1}}$	$\mathrm{E_{W1}}$	$\mathrm{F_{W1}}$	$\mathrm{A_{M1}}$	$\mathrm{B_{M1}}$	$\mathrm{C_{M1}}$	$\mathrm{D_{M1}}$	$\mathrm{E_{M1}}$	$\mathrm{F_{M1}}$
θ (1,2,3,4)	1	0.0	0.0	0.4	−0.4	−0.2	−1.9	−0.2	−1.0	1.1	−0.9	−0.8	−1.9
	2	2.1	−0.7	3.2	0.4	−2.6	−0.8	2.3	−0.5	3.2	0.4	−2.4	−0.6
θ (2,3,4,5)	1	−0.3	0.8	−0.3	−0.1	0.4	1.6	−0.1	0.5	−0.7	0.3	0.7	1.9
	2	−1.6	0.2	−2.4	−0.3	2.0	0.8	−1.7	0.2	−2.4	−0.4	1.9	0.5
θ (3,4,5,6)	1	−0.5	−0.1	0.1	0.3	−0.1	0.1	−0.1	0.7	0.0	0.4	0.0	0.0
	2	1.3	0.3	1.4	0.2	−1.3	0.0	1.4	0.3	1.5	0.2	−1.2	0.0
θ (4,5,6,7)	1	−178.3	178.8	180.0	180.0	179.7	178.5	−179.2	178.3	180.0	179.6	179.5	178.4
	2	178.8	179.7	179.0	180.0	−179.2	179.1	178.7	179.6	178.9	179.9	−179.3	179.5
θ (13,14,7,6)	1	13.4	3.8	–	–	–	–	4.9	11.8	–	–	–	–
	2	3.3	8.9	–	–	–	–	0.0	4.0	–	–	–	–
θ (14,13,11,1)	1	4.9	18.6	–	–	9.0	11.5	1.7	13.0	–	–	6.2	6.6
	2	7.7	2.5	–	–	7.8	2.1	4.6	−3.1	–	–	4.6	−3.5
θ (13,14,8,2)	1	–	–	1.0	3.3	5.1	20.2	–	–	−6.0	5.6	−2.2	19.6
	2	–	–	0.4	4.0	4.3	8.8	–	–	−3.2	0.0	0.9	4.4
θ (14,13,12,3)	1	–	–	6.5	−2.6	–	–	–	–	4.0	−11.9	–	–
	2	–	–	7.3	3.8	–	–	–	–	5.0	−2.0	–	–

1 B3LYP/$6-31+G$(d); *2 MP*2/$6-31+G$(d) to two protic molecules. The next limitation is the method – it should be well chosen, conformable to the molecular size and leading to results comparable with experiment. These two major limitations determined the optimum method/basis set we chose here.

In Fig. 1 are compared the H-bond lengths of all binary supersystems in the ground state, at standard conditions. As one can see in the supersystems C_{W1} and C_{M1} the difference between the H-bond lengths is the smallest and these bonds are the shortest ones. With respect to the 2- and 6-hydroxo-uracil monomers

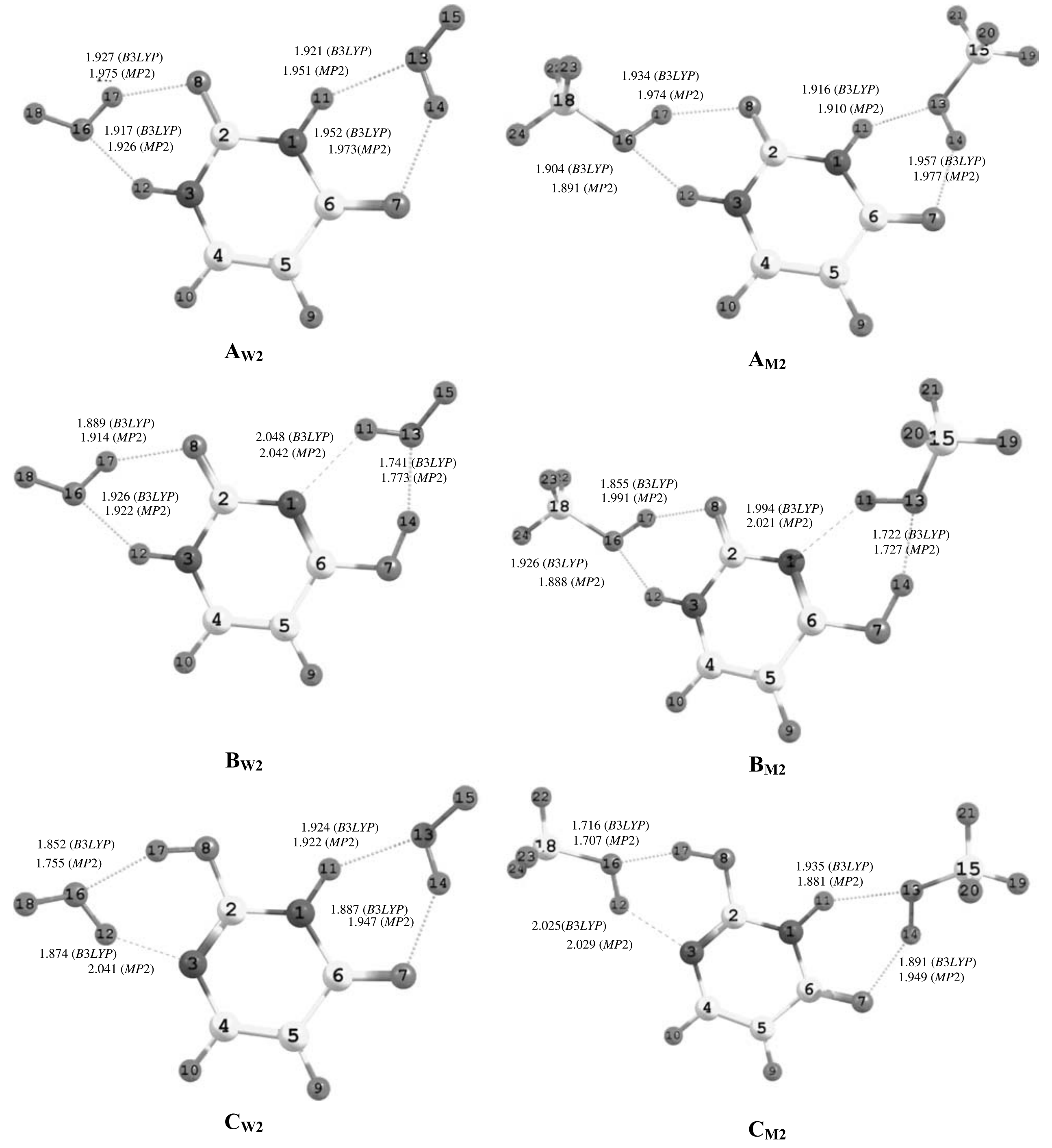

A_{W2} A_{M2}

B_{W2} B_{M2}

C_{W2} C_{M2}

Fig. 2 Optimized structures of the ternary supersystems

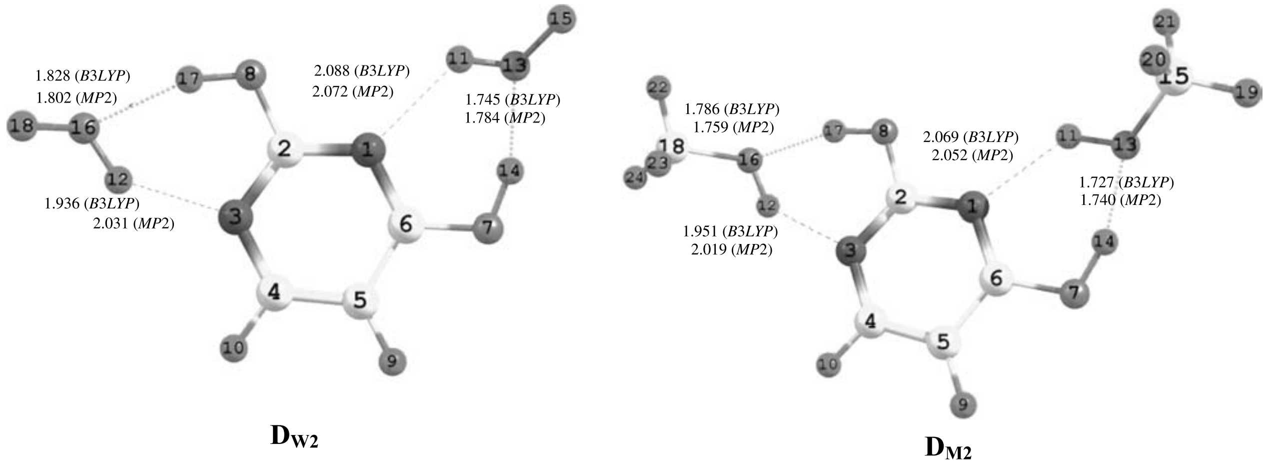

D_{W2} D_{M2}

Fig. 2 (*continued*)

the shortest H-bond was calculated in the F_{M1} supersystem. The last seems to be the most favorable way for H-bonding as compared to all twelve binary complexes. However, as seen above, the supersystems F_{W1} and F_{M1} have the highest energies. This discrepancy can be explained with the strength of the remaining H-bonds in the F_{W1} and F_{M1} supersystems, which are comparatively long. The stability of the supersystems can be find out better through their bonding and thermodynamic parameters that will be discussed below. Several dihedral angles are listed in Table 2 in order to explore the planarity of the uracil monomer and the water/methanol atoms involved in H-bonding.

There is no structure that has completely planar geometry. The values of the last four dihedral angles listed in Table 2 show that the intermolecular H-bonding between the monomers through two H-bonds does not occur in one plane. Thus, the intermolecular H-exchange (see below) is expected to be hindered by steric reasons. It is known that the proton transfer occurring out of the molecular plane leads to an increase of the energy barrier [23]. The non-H-bonded proton (water) and carbon (methanol) deviated considerably from the molecular plane.

Eight H-bonded supersystems (Fig. 2) between two water molecules and uracil, and two methanol

Table 3 Dihedral angles of supersystems two molecules water/methanol – uracil

Dihedral angle/deg	Level	A_{W2}	B_{W2}	C_{W2}	D_{W2}	A_{M2}	B_{M2}	C_{M2}	D_{M2}
θ (1,2,3,4)	1	0.3	0.0	−1.7	0.0	0.7	1.7	0.3	−1.0
	2	2.8	0.9	0.5	0.3	3.0	1.1	0.6	0.3
θ (2,3,4,5)	1	−0.6	0.7	0.4	0.1	−0.7	−0.9	−0.1	0.2
	2	−2.1	−0.8	−0.3	−0.3	−2.3	−0.9	−0.4	−0.3
θ (3,4,5,6)	1	−0.3	0.0	0.4	0.1	−0.2	−0.4	−0.3	0.6
	2	1.4	0.4	0.4	0.1	1.6	0.4	0.5	0.2
θ (4,5,6,7)	1	−178.3	178.6	−179.6	179.8	−178.9	−179.1	−179.3	179.4
	2	178.9	180.0	179.6	−179.9	178.7	179.9	179.5	179.9
θ (13,14,7,6)	1	13.1	3.1	8.8	4.2	6.9	2.4	2.5	6.8
	2	2.8	9.0	1.8	7.9	−0.6	4.2	−1.6	2.5
θ (14,13,11,1)	1	4.4	18.6	3.4	11.2	1.2	−2.1	−3.3	2.9
	2	7.2	2.4	7.0	2.8	4.1	−3.3	4.1	−3.0
θ (17,16,12,3)	1	7.4	8.2	−12.2	0.8	4.5	1.0	6.6	−9.1
	2	7.2	7.0	3.6	3.8	4.6	4.0	−2.3	−2.6
θ (16,17,8,2)	1	2.3	3.3	9.3	−1.0	−3.7	−12.1	7.6	4.1
	2	−0.3	−1.0	3.1	2.0	−4.6	−5.5	−1.1	−3.6

1 B3LYP/6 − 31 + *G*(d); *2 MP2*/6 − 31 + *G*(d) molecules and uracil were also investigated at the DFT and *MP*2 level of theory. According to the data listed in Table 1 the supersystems A_{W2} and A_{M2} have the lowest energy as compared to all ternary systems, which follow the energy pattern: $A_{W/M2} < B_{W/M2} < C_{W/M2} < D_{W/M2}$ (*B3LYP*). The data from Table 1 show that according to the *MP*2 calculations the second and third positions of the energy pattern in the methanol containing supersystems are occupied by the supersystems C_{M2} and B_{M2}, with an energy difference of 0.2 kJ mol^{-1}.

The *Onsager* model for an environment modeling led to the reduction of the energies of the ternary supersystems on the average of 5 kJ mol^{-1}.

Comparing the H-bond lengths in Figs. 1 and 2 one can see that the additional bonding of the second protic molecule (as a "second" molecule of water or methanol it is designated that one having a larger numeration of the atoms) causes a slight shortening of the H-bonds between oxo-uracil and water/methanol (according to *B3LYP* results). Conversely, in the 6-hydroxo-uracil the H-bonds get longer, with one exception: the bond H11 ⋯ N1 gets 0.059 Å shorter. It is interesting to mention also that the inclusion of the second protic molecule does not change the space arrangement of atoms (Table 3), in particular for the uracil ring.

Thermodynamic and bonding parameters of the complexes

The calculated bonding and thermodynamic parameters of all supersystems are given in Tables 4 and 5.

The data show that the most stable binary supersystems are F_{W1} and F_{M1} despite the highest energies calculated for them (see the energy patterns given above). The bonding and thermodynamic analysis should be taken as a more accurate since it gives the stability of the supersystems from the point of view of the H-bond strengths. That is why only the calculated energies are not enough for doing reasonable conclusions (as has done in Ref. [14]) about stability of one H-bonded complex. For example the lowest energy of the supersystems C_{W1} and C_{M1} may be a result of the high stability of the oxo-uracil monomer (it was mentioned that the oxo-uracil

Table 4 Bonding parameters and thermodynamic parameters of the complex formations/kJ mol^{-1}. K_p – equilibrium constant of complex formation (Pa^{-1} for dimers and Pa^{-2} for trimers)

Supersystem	Bonding parameters				Thermodynamic parameters			
	ΔE_b	ΔE_{int}	ΔE	ΔBSSE	ΔH^0_{298}	ΔG^0_{298}	$T\Delta S^0_{298}$	K_p
Binary supersystems								
A_{W1}	−37.6	−39.9	−42.2	4.6	−32.6	7.7	−40.3	0.0447
B_{W1}	−50.2	−52.0	−56.4	6.2	−44.8	−4.8	−40.0	6.9405
C_{W1}	−44.9	−47.3	−49.4	4.5	−39.7	1.0	−40.7	0.6679
D_{W1}	−51.3	−53.7	−57.8	6.5	−45.9	−3.5	−42.4	4.1059
E_{W1}	−35.0	−37.5	−39.5	4.5	−30.3	9.5	−39.8	0.0216
F_{W1}	−58.9	−60.1	65.4	6.4	−52.7	−10.3	−42.4	63.8985
A_{M1}	−38.0	−39.4	−41.5	3.5	−32.5	8.1	−40.6	0.0380
B_{M1}	−53.2	−53.9	−58.9	5.8	−46.8	−5.0	−41.8	7.5241
C_{M1}	−45.1	−46.4	−48.7	3.6	−39.1	1.4	−40.5	0.5683
D_{M1}	−53.0	−53.7	−59.1	6.1	−46.3	−3.5	−42.8	4.1069
E_{M1}	−35.3	−36.8	−38.8	3.5	−29.8	10.1	−39.9	0.0170
F_{M1}	−61.0	−60.9	−66.9	5.9	−53.9	−11.6	−42.3	107.9862
Ternary supersystems								
A_{W2}	−83.0	−88.0	−92.2	9.3	−73.0	8.1	−81.1	0.0380
B_{W2}	−99.3	−102.8	−110.2	10.8	−87.8	−6.6	−81.2	14.3521
C_{W2}	−90.2	−94.7	−100.8	10.6	−79.7	2.5	−82.2	0.3646
D_{W2}	−90.4	−95.9	102.5	12.1	−80.7	2.2	−82.9	0.4115
A_{M2}	−83.7	−86.5	−90.9	9.2	−72.2	9.2	−81.4	0.0244
B_{M2}	−102.9	−104.8	−112.7	9.8	−90.0	−7.0	−83.0	16.8668
C_{M2}	−96.6	−98.7	−105.6	8.9	−84.7	−1.6	−83.1	1.9075
D_{M2}	−93.3	−96.4	−104.7	11.4	−82.0	1.4	−80.6	0.5683

Table 5 Bonding parameters (kJ mol^{-1}) between one monomer and another pair of monomers in the frames of one ternary supersystem

Supersystem	$\Delta E'_b$			$\Delta E'_{\mathrm{int}}$			$\Delta E'$		
	1	2	3	1	2	3	1	2	3
A_{W2}	−45.6	−38.3	−82.4	−48.0	−40.7	−88.0	−50.3	−42.9	−91.5
B_{W2}	−48.7	−49.5	−100.4	−50.8	−51.3	−102.8	−53.4	−55.7	−111.3
C_{W2}	−45.6	−43.7	−91.0	−47.7	−41.0	−94.7	−51.6	−48.4	−101.7
D_{W2}	−44.4	−47.3	−89.9	−46.8	−50.1	−95.9	−50.4	−53.7	−101.9
A_{M2}	−45.8	−38.7	−83.1	−47.1	−40.1	−86.5	−49.5	−42.3	−90.2
B_{M2}	−48.8	−53.0	−103.4	−50.9	−54.7	−104.8	−52.6	−59.1	−113.7
C_{M2}	−51.8	−43.7	−97.2	−52.7	−45.0	−98.7	−57.3	−47.1	−100.2
D_{M2}	−45.5	−49.7	−92.7	−46.2	−51.3	−96.4	−51.3	−55.2	−104.0

1 (*U*-*W*1/*M*1) ··· *W*2/*M*2; *2* (*U*-*W*2/*M*2) ··· *W*1/*M*1; *3* (*W*1/*M*1–*W*2/*M*2) ··· *U*

monomer has the lowest energy). However, it does not mean that these binary supersystems have the strongest H-bonds. As seen (Table 4) these supersystems have moderate stability. Therefore, the careful bonding and thermodynamic analysis refuted the finding of *Bao et al.* [14] concerning the highest stability of C_{W1} supersystem.

The supersystems F_{W1} and F_{M1} have the largest negative bonding and interaction energies. Furthermore, equilibrium of their formation in the gas phase is shifted in a forward direction ($K_p \gg 1$, ΔG^0_{298} has the largest negative value). The next binary complexes follow the stability pattern (composed by ΔG^0_{298} values): $F_{W/M1} < B_{W/M1} < D_{W/M1} < C_{W/M1} < A_{W/M1} < E_{W/M1}$ (*B3LYP*). The formations of supersystems F_{W1} and F_{M1} are characterized with the largest steric changes ($|T\Delta S^0_{298}|$) and a considerable heat effect. The binary complex formations are exothermic, accompanied with large steric effects as well. The equilibrium of the complex formations $A_{W/M1}$, $C_{W/M1}$, and $E_{W/M1}$ are shifted in the reverse direction. In general, all methanol containing binary complexes are more stable than the water containing ones.

The bonding and thermodynamic analysis of the ternary supersystems showed that the complexes B_{W2} and B_{M2} are the most stable ones having bonding and thermodynamic parameters considerably distinguished from all remaining. The equilibrium of the complex formations of B_{W2} and B_{M2} is shifted in a forward direction. In all other cases it is moved in a reverse direction. The ΔE_b values explicitly show that the complex B_{M2} is more stable than B_{W2} one. Furthermore, all methanol containing ternary supersystems are more stable than the water containing ones.

In Table 5 are presented the bonding parameters between one monomer and another pair of monomers of a given ternary supersystem. These values could serve for an estimation of the contribution of each protic molecule (water or methanol) to the bonding and interaction energy. Therefore, in the supersystems $A_{W/M2}$, and $C_{w/M2}$ the largest part of the bonding energy is due to the "second" protic molecule, while in the supersystems $B_{W/M2}$, and $D_{W/M2}$ – to the "first" one.

Ground state intermolecular proton transfers

In order to investigate the reaction mechanism of the solvent-assisted (intermolecular-) proton transfers we optimized the structures of the transition states. They are presented in Fig. 3.

Each transition state was found as a first order saddle point on the reaction potential energy surface. It means that the given transition state is a maximum-energy point along the reaction coordinate, and a minimum-energy point in all other directions. In the vibration spectrum of each transition state was calculated one imaginary vibrational mode, whose form describes the intermolecular proton exchange between uracil and water or methanol.

Regarding the intermolecular proton transfers in the binary systems, one can see (in Fig. 3) that in the transition states a breaking of one H-bond and a formation of another one is occurred. This simultaneous proton exchange would lead to lower energy barriers as compared to the intramolecular proton transfers [26]. The barriers in these cases have to be lower than the absolute values of the bonding energies of the supersystems. It means that during the proton transfers all complexes stay stable systems with a minimal waste of energy. If the energy barriers are higher than the absolute values of the bond-

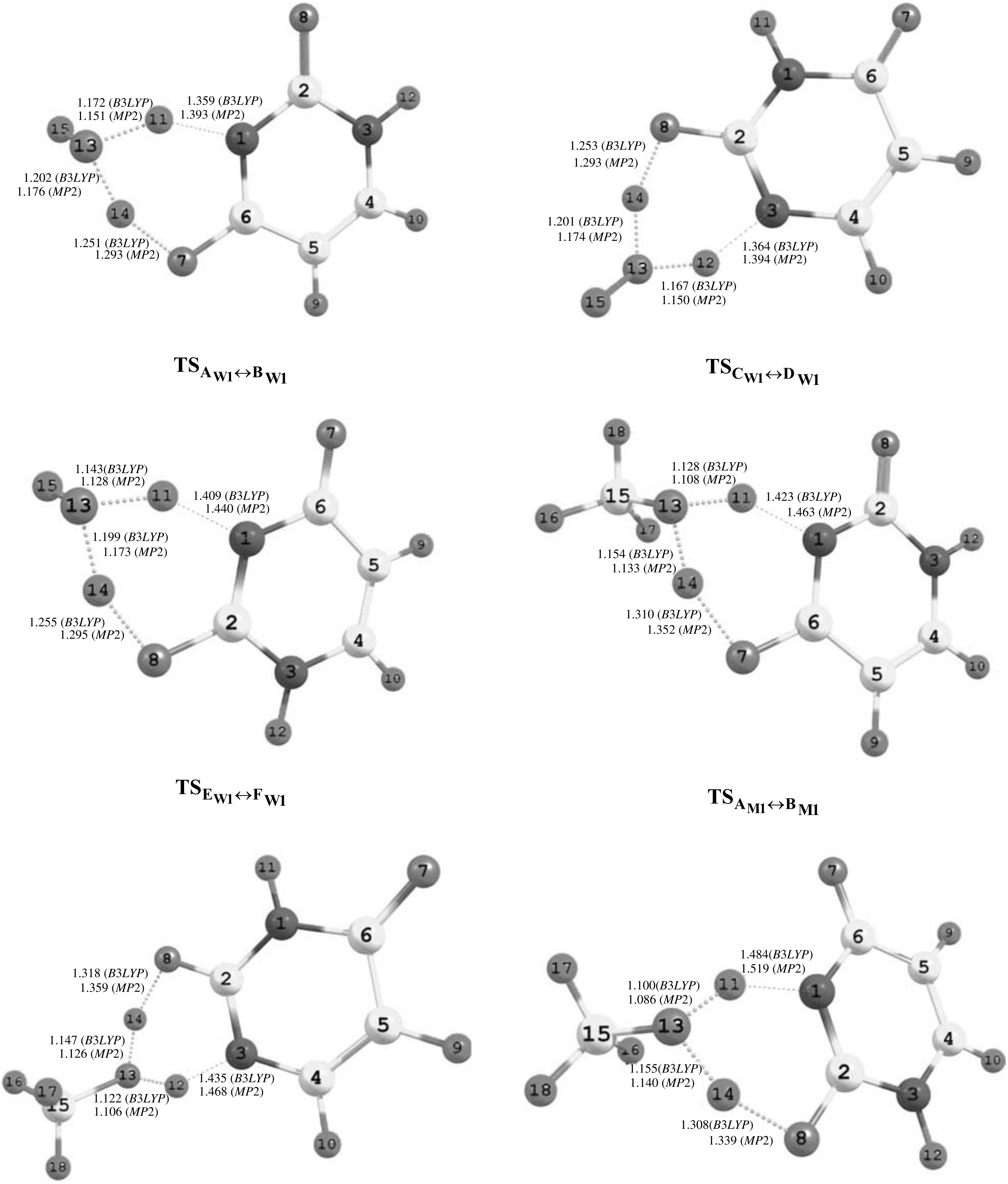

$\mathbf{TS}_{\mathbf{A}_{\mathbf{W1}}\leftrightarrow\mathbf{B}_{\mathbf{W1}}}$ $\mathbf{TS}_{\mathbf{C}_{\mathbf{W1}}\leftrightarrow\mathbf{D}_{\mathbf{W1}}}$

$\mathbf{TS}_{\mathbf{E}_{\mathbf{W1}}\leftrightarrow\mathbf{F}_{\mathbf{W1}}}$ $\mathbf{TS}_{\mathbf{A}_{\mathbf{M1}}\leftrightarrow\mathbf{B}_{\mathbf{M1}}}$

$\mathbf{TS}_{\mathbf{C}_{\mathbf{M1}}\leftrightarrow\mathbf{D}_{\mathbf{M1}}}$ $\mathbf{TS}_{\mathbf{E}_{\mathbf{M1}}\leftrightarrow\mathbf{F}}$

Fig. 3 Optimized structures of the transition states (TS) of the intermolecular proton transfers ing energies, this would cause a decomposition of the complexes during the intermolecular proton transfers.

Concerning the ternary systems (Figs. 2 and 3) one can see that the intermolecular proton transfers cause change in the H-bond lengths (strengths) between

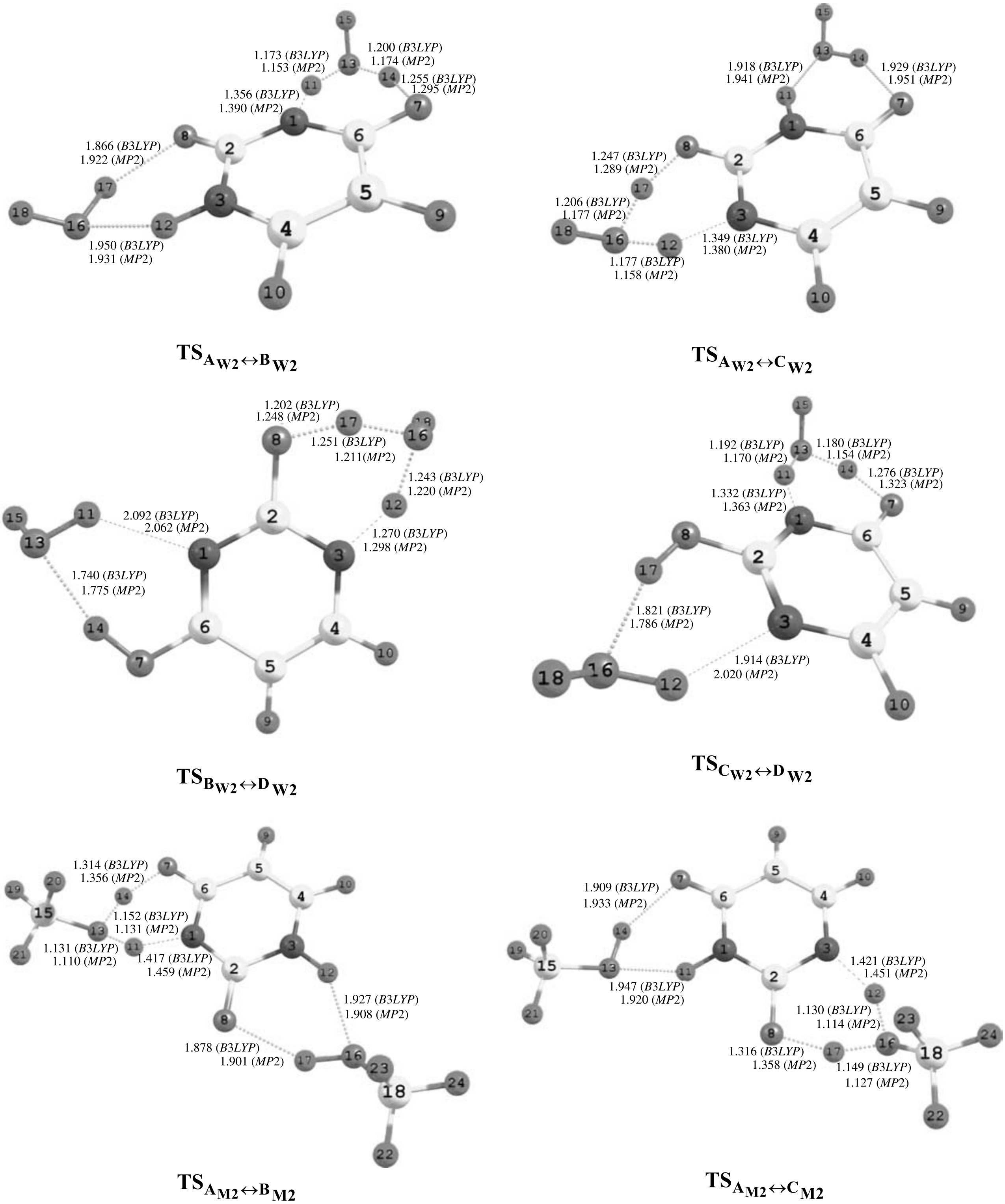

$\mathrm{TS}_{\mathrm{A}_{\mathrm{W2}}\leftrightarrow \mathrm{B}_{\mathrm{W2}}}$ $\mathrm{TS}_{\mathrm{A}_{\mathrm{W2}}\leftrightarrow \mathrm{C}_{\mathrm{W2}}}$

$\mathrm{TS}_{\mathrm{B}_{\mathrm{W2}}\leftrightarrow \mathrm{D}_{\mathrm{W2}}}$ $\mathrm{TS}_{\mathrm{C}_{\mathrm{W2}}\leftrightarrow \mathrm{D}_{\mathrm{W2}}}$

$\mathrm{TS}_{\mathrm{A}_{\mathrm{M2}}\leftrightarrow \mathrm{B}_{\mathrm{M2}}}$ $\mathrm{TS}_{\mathrm{A}_{\mathrm{M2}}\leftrightarrow \mathrm{C}_{\mathrm{M2}}}$

Fig. 3 (*continued*)

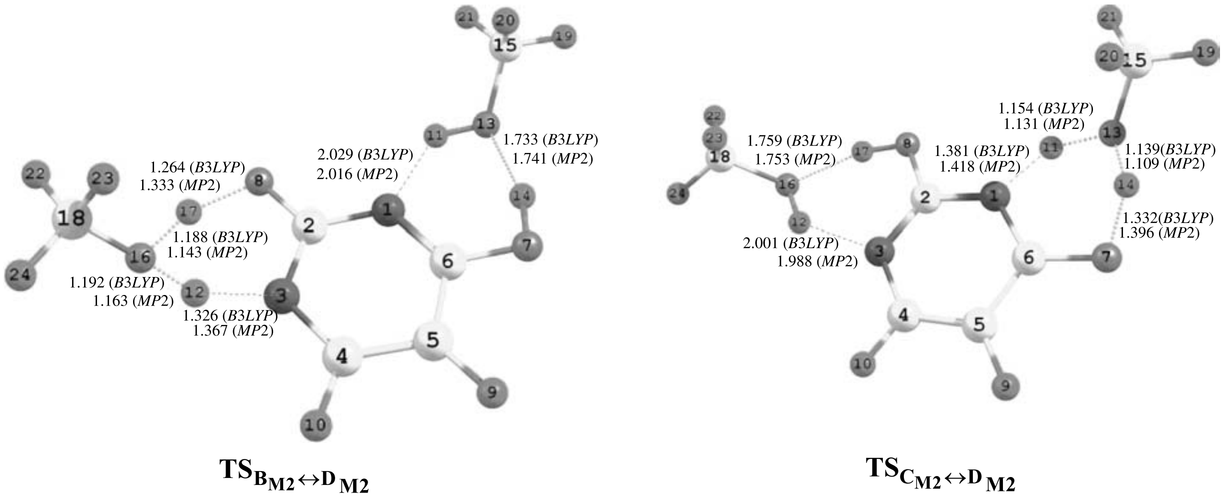

$TS_{B_{M2} \leftrightarrow D_{M2}}$ $TS_{C_{M2} \leftrightarrow D_{M2}}$

Fig. 3 (*continued*)

uracil and the water/alcohol molecule, which is not involved in the proton exchange.

From the point of view of chemical kinetics, the water and methanol molecules could be examined as catalysts, which facilitate the proton exchange in uracil. It should be expected that lower energy barriers are obtained for water and methanol assisted proton transfers as compared to the intramolecular proton migration in uracil. There is no doubt that a competition exists between water and methanol molecules as catalysts. Better catalysts would be those that lessen in a greater extent the energy barriers of the proton transfers in uracil. The calculated values of the energy barriers are listed in Table 6.

The *B3LYP* and *MP2* calculations showed that the methanol molecule reduces in a greater extent (*B3LYP*, ~4 kJ mol^{-1}) the energy barrier as compared to the water molecule. In other words, the methanol molecule can provoke easier point mutations in *RNA* molecule [24, 25].

The data show that the energy barriers of the water and methanol assisted proton transfers in uracil are more than 50% reduced than those of intramolecular proton transfer, given in Ref. [26]. For ex-

Table 6 Energy barriers (ε) and thermodynamic parameters (*B3LYP*) of the ground state intermolecular proton transfers/kJ mol^{-1}

Proton transfer	*B3LYP*				*MP2*		ΔH^0_{298}	ΔG^0_{298}	$T\Delta S^0_{298}$
	1	2	1*	2*	1	2			
$A_{W1} \rightleftarrows B_{W1}$	88	44	86	39	97	56	42.4	42.5	−0.1
$C_{W1} \rightleftarrows D_{W1}$	90	44	88	41	97	54	44.4	47.0	−2.6
$E_{W1} \rightleftarrows F_{W1}$	102	37	99	37	108	46	63.8	65.9	−2.1
$A_{M1} \rightleftarrows B_{M1}$	83	42	90	43	84	45	40.2	41.9	−1.7
$C_{M1} \rightleftarrows D_{M1}$	84	40	77	31	84	43	43.4	46.5	−3.1
$E_{M1} \rightleftarrows F_{M1}$	96	32	96	35	94	35	62.1	64.0	−1.9
$A_{W2} \rightleftarrows B_{W2}$	86	45	90	45	95	57	39.7	40.3	−0.6
$A_{W2} \rightleftarrows C_{W2}$	87	42	88	40	95	56	43.9	45.8	−1.9
$B_{W2} \rightleftarrows D_{W2}$	74	58	74	58	81	70	16.0	18.7	−2.7
$C_{W2} \rightleftarrows D_{W2}$	70	58	70	57	79	69	11.8	13.2	−1.4
$A_{M2} \rightleftarrows B_{M2}$	82	44	85	47	82	46	36.8	38.8	−2.0
$A_{M2} \rightleftarrows C_{M2}$	83	43	78	40	82	46	38.2	40.5	−2.3
$B_{M2} \rightleftarrows D_{M2}$	72	54	73	53	71	61	16.8	18.3	−1.5
$C_{M2} \rightleftarrows D_{M2}$	69	54	73	54	67	57	15.4	16.6	−1.2

1 Forward; *2* reverse; *1** forward, including solvent energy; *2** reverse, including solvent energy ample the forward transformations $A_{W/M1} \rightleftarrows B_{WM/1}$ and $C_{W/M1} \rightleftarrows D_{WM/1}$ without catalysts (intramolecularly) pass through energy barriers of 184 and 189 kJ mol^{-1} in the gas phase [26]. Obviously, the catalysts (water, methanol) change the mechanism of proton exchange and lead to the increase of the reaction rate. It is seen also that the inclusion of the second protic molecule in one supersystem does not change significantly the energy barriers of the proton transfers, *i.e.*, the assisted proton transfers in uracil are not influenced on the number of the H-bonded molecules to the uracil monomer.

With regard to the solvent influence one can see that the reductions of the energy barriers of the forward reactions are on the average 2 kJ mol^{-1}. Furthermore, some of the forward reactions have higher energy barriers including solvent energy, found by *Onsager* model. Obviously, the continuum models can not be useful when studying the assisted proton transfers because their nature reveals the discrete interactions solvent-dissolved molecule.

The careful analysis of the thermodynamic parameters of the proton transfers shows (Table 6) that the forward transformations are thermodynamically disfavored. They all occur with insignificant steric changes (the values $T\Delta S^0_{298}$ are small) but with considerable energetic changes (large ΔH^0_{298} values) as endothermic reactions. That means that the reactants are more stable than products, and the transition states are product-like ("late") according to the *Leffler-Hammond* postulate [27, 28].

Conclusions

The stability of H-bonded systems uracil-(H_2O/CH_3OH)$_n$ ($n = 1, 2$) and intermolecular H-transfer in uracil, assisted by water and methanol molecules were studied at the *B3LYP* and *MP2* levels of theory using the basis set $6-31+G$(d). The major contributions of the investigation can be summarized as follows:

1) In contrast to previously published investigations [14] the oxo-uracil containing supersystems were not found to be the most stable ones (especially C_{W1}, C_{M1}, A_{W2}, and A_{M2}, which have the lowest energy). The thermodynamic and bonding analysis predicted the dimers F_{W1} and F_{M1} as well as trimers B_{W2} and B_{M2} (all containing hydroxo-uracil) to be the systems with the highest stability.

2) It was established that the methanol molecule provokes a larger reduction of the energy barrier of the intermolecular proton exchange reactions than the water molecule. The obtaining of another tautomer of uracil distinguished from the oxo-uracil (normally this tautomer is included in the *RNA* molecule [24, 25]) could cause mutations. Thus, methanol could better catalyze mutations than water.

Methods

The optimizations of the supersystems at the *B3LYP*/ $6-31+G$(d) theoretical level were carried out with the Gaussian 98 program [30], whereas those at the *MP2*/ $6-31+G$(d) level – by means of the GAMESS [31] program package. The basis set $6-31+G$(d) has shown good accuracy and comparatively low cost in computational time in calculating H-bonds and energy parameters of *DNA* bases and other bioorganic compounds [32–34].

The optimizations were performed in the ground state by standard gradient procedure with no symmetry restrictions. Subsequent frequency calculations were carried out to prove that the resulting stationary points are real energy minima (without imaginary frequencies in their vibration spectra). It has been demonstrated that the *B3LYP* functional yielded accurate normal mode frequencies for intermolecular normal modes compared with experiment [35]. Each transition state located between two minima was found by using the QST2 procedure (included in Gaussian 98) or by means of the SADPOINT one (included in GAMESS).

Bonding energies (ΔE_b) and BSSE for each supersystem were estimated according to the equations [36–38]

$$\Delta E_b = E_{SS} - \sum_{i=1}^{n} E'_{m_i}, \Delta(\mathrm{BSSE}) = \sum_{i=1}^{n} (E^{SP}_{m_i} - E'_{m_i}),$$
$$\text{and} \quad \Delta E'_b = E_{SS} - (E'_{m_i} + E'_d),$$

where E_{SS} is the energy of the complex (supersystem); E'_{m_i} is the energy of i-th monomer in the supersystem calculated with "ghost" orbitals of the remaining monomer(s); $E^{SP}_{m_i}$ are the energies of the individual monomers frozen in their aggregate geometries, found by single-point calculations; E'_d is the energy of the binary system (in the frames of one ternary system), whose energy was calculated including the "ghost" orbitals of the remaining monomer.

The interaction energy was calculated by the equations:

$$\Delta E_{\mathrm{int}} = E_{SS} - \sum_{i=1}^{n} E_{m_i}, \quad \text{and} \quad \Delta E'_{\mathrm{int}} = E_{SS} - (E_{m_i} + E_d),$$

where E_{m_i} and E_d are the energy of isolated monomers and binary systems, found by the optimizations.

The energies ΔE and $\Delta E'$ were calculated using the equations:

$$\Delta E = E_{SS} - \sum_{i=1}^{n} E^{SP}_{m_i}, \quad \text{and} \quad \Delta E'_{\mathrm{int}} = E_{SS} - (E^{SP}_{m_i} + E^{SP}_d).$$

The X-ray powder spectra of uracil (FLUKA), and uracil precrystallized from methanol and water were recorded on a TUR-MA-62 apparatus, working tension of 32 kV, Cu-anticathode, $\lambda_{\alpha 1} = 1.5405$ Å, $\lambda_{\alpha 2} = 1.5443$ Å, $\bar{\lambda} = 1.5424$ Å.

Small amounts of uracil were hot-dissolved in ~70–80 cm^3 water/methanol until a saturated solution is obtained. After boiling to the volume of 20 cm^3 the solutions were cooled several hours at room temperature. The white crystals of uracil were filtered and left several days at room temperature to dry.

Acknowledgements

We thank the National Science Fund (Ministry of Education and Science of Bulgaria) for the financial support (Project "Young Scientists – Chemistry – 1504").

References

1. Hobza P, Sponer J (1999) Chem Rev 99:3247
2. van Mourik T, Benoit DM, Price SL, Clary DC (2000) Phys Chem Chem Phys 2:1281
3. Leszczynski J (1992) J Phys Chem 96:1649
4. Delchev VB, Mikosch H (2006) J Mol Mod 12:229
5. Portalone G, Ballirano P, Maras A (2002) J Mol Str 608:35
6. Cysewski P (2005) J Mol Str Theochem 714:29
7. Sowerby SJ, Edelwirth M, Heckl WM (1998) J Phys Chem B 102:5914
8. Nir E, Grace L, Brauer B, de Vries MS (1999) J Am Chem Soc 121:4896
9. Mons M, Dimicoli I, Piuzzi F, Tardivel B, Elhanine M (2002) J Phys Chem A 106:5088
10. Piuzzi F, Mons M, Dimicoli I, Tardivel B, Zhao Q (2001) Chem Phys 270:205
11. Poznanski J (2005) J Mol Liq 121:15
12. Nowak MJ, Lapinski L, Bienko DC, Michalska D (1997) Sectrochim Acta A 53:855
13. Latajka Z, Ratajczak H, Zeegers-Huyskens Th, Scheiner S (1991) J Mol Str THEOCHEM 235:409
14. Bao X, Sun H, Wong N-B, Gu J (2006) J Phys Chem B 110:5865
15. Kabeláč M, Hobza P (2007) Phys Chem Chem Phys 9:903
16. Lill MA, Hutter MC, Helms V (2000) J Phys Chem A 104:8283
17. Parry GS (1954) Acta Cryst 7:313
18. Stewart RF, Jensen LH (1967) Acta Cryst 23:1102
19. Gu J, Leszczynski J (1999) J Phys Chem A 103:2744
20. Mebel AM, Morokuma K, Lin CM (1995) J Chem Phys 103:7414
21. Civcir Pü (2000) J Mol Str THEOCHEM 532:157
22. van Mourik T, Emson LE (2002) Phys Chem Chem Phys 4:5863
23. Delchev VB (2004) J Struct Chem 45:602
24. Knippers R (1997) Molekulare Genetik. Thieme, Stuttgart
25. Kryachko ES (2002) Int J Quantum Chem 90:910
26. Shterev IG, Delchev VB (2006) Scientific works of University of Plovdiv 34:105
27. Hammond GS (1955) J Am Chem Soc 77:334
28. Leffler JE (1953) Science 117:340
29. Foresman JB, Frisch Æ (1996) Electronic Chemistry with Electronic Structure Methods. Gaussian Inc, p 69
30. Frisch MJ, Trucks GW, Schlegel HB, Scuseria GE, Robb MA, Cheeseman JR, Zakrzewski VG Jr, Montgomery JA, Stratmann RE, Burant JC, Dapprich S, Millan JM, Daniels AD, Kudin KN, Strain MC, Farkas O, Tomasi J, Barone V, Cossi M, Cammi R, Mennucci B, Pomelly C, Adamo C, Clifford S, Ochterski J, Petersson GA, Ayala PY, Cui Q, Morokuma K, Malick DK, Rabuck AD, Raghavachari K, Foresman JB, Cioslowski J, Ortiz JV, Baboul AG, Stefanov BB, Liu G, Liashenko A, Piskorz P, Komaromi I, Gomperts R, Martin RL, Fox DJ, Keith T, Al-Laham MA, Peng CY, Nanayakkara A, Gonzalez C, Challacombe M, Gill PMW, Johnson B, Chen W, Wong MW, Andres JL, Gonzalez C, Head-Gordon M, Replogle ES, Pople JA (1998) Gaussian 98, A.3., Revision, Gaussian Inc., Pittsburgh PA
31. Schmidt MW, Baldridge KK, Boatz JA, Elbert ST, Gordon MS, Jensen JH, Koseki S, Matsunaga N, Nguyen KA, Su S, Windus TL, Dupuis M, Montgomery JA (1993) J Comput Chem 14:1347
32. Li X, Cai Z, Sevilla MD (2002) J Phys Chem A 106:9345
33. Li X, Cai Z, Sevilla MD (2001) J Phys Chem B 105:10115
34. van Mourik T (2004) Phys Chem Chem Phys 6:2827
35. Müller A, Losada M, Leutwyler S (2004) J Phys Chem A 108:157
36. Boys SF, Bernadi F (1970) Mol Phys 19:553
37. Hobza P, Zahradnik R (1989) Intermolecular Complexes. Mir Press, Moscow, p 36 (in Russian)
38. Simon S, Duran M, Dannenberg JJ (1999) J Phys Chem A 103:1640